High-temperature neutron diffraction study of $La_{2-x}Sr_xCoO_4$: Correlation between structure and transport properties

Cristina Tealdi,[1,*] Chiara Ferrara,[1] Lorenzo Malavasi,[1] Piercarlo Mustarelli,[1] Clemens Ritter,[2] Gaetano Chiodelli,[3] and Yuri Antonio Diaz-Fernandez[4]

[1]*Dipartimento di Chimica Fisica, Università di Pavia, Viale Taramelli 16, 27100 Pavia, Italy*

[2]*Institute Laue-Langevin, Boite Postale 156, F-38042 Grenoble, France*

[3]*Sezione di Pavia, IENI/CNR, Viale Taramelli 16, 27100 Pavia, Italy*

[4]*Dipartimento di Chimica Generale, Università di Pavia, Viale Taramelli 12, 27100 Pavia, Italy*

(Received 2 September 2010; published 17 November 2010)

This study focuses on the characterization of the structural and transport properties of the $La_{2-x}Sr_xCoO_4$ solid solution. The wide temperature range investigated (30–750 °C) has been chosen in view of the potential applications of this class of materials both as catalysts and as cathodes for intermediate temperature solid oxide fuel cells. The trend vs temperature of several structural parameters, as well as of the transport properties, for the $La_{2-x}Sr_xCoO_4$ series is complex and strongly dependent on composition. A possible correlation between the structural and the transport properties, based on changes in the average oxidation and spin state of the Co ions, is proposed.

DOI: 10.1103/PhysRevB.82.174118 PACS number(s): 61.05.fm, 82.33.Pt

I. INTRODUCTION

K_2NiF_4-type oxides have been the subject of intense research since the discovery of superconductivity in the La_2CuO_4 system.[1,2] Recently, these oxides are gathering a renewed attention as catalysts[3] and cathode materials[4] for high-temperature solid oxide fuel cells. Their interesting electrochemical properties derive from the coupling between crystal and defect structure properties and may be tailored to specific applications by means of chemical doping.[5]

Compounds in the system $La_{2-x}Sr_xCoO_{4\pm\delta}$ belong to the family of oxides which crystallize in the tetragonal K_2NiF_4-type structure (Fig. 1). Within this structure, the CoO_6 octahedra are connected to form a two-dimensional network by corner-sharing oxygen atoms. These layers, which are similar to those found in the perovskite structure, are separated by (La,Sr)O slabs with the rocksalt structure; La and Sr (ideally sharing the same crystallographic site, named A in the following) are nine coordinated to oxygen.

The oxygen nonstoichiometry in the $La_{2-x}Sr_xCoO_{4\pm\delta}$ system can be, in principle, modulated as a function of the alkaline-earth doping on the A site. In practice, charge neutrality is easily accomplished by variation in the Co oxidation state.[6] In addition, Co ions can exist in three spin states, i.e., low spin (LS), intermediate spin (IS), and high spin (HS), depending on the subtle coupling between crystal-field effects and on-site Coulomb interaction.

The electronic configuration of Co at room temperature (RT) in the $La_{2-x}Sr_xCoO_{4\pm\delta}$ system is at present still a matter of discussion. For example, Co^{3+} in $LaSrCoO_4$ is believed to be present in the IS state[7–9] or as a mixture of LS and HS.[10,11] Based on magnetic measurements, it has been proposed that the spin state of Co^{3+} in the series $La_{2-x}Sr_xCoO_{4\pm\delta}$ changes from HS to IS along with the composition when $x>0.8$,[8] although Co^{3+} has been shown to be in the LS state[12] or the IS state[13] fox $x=0.5$. At this Sr doping a charge ordered (CO) state has been found with a simple checkerboard-type arrangement of Co^{2+}/Co^{3+} in the tetragonal plane with the CO persisting to at least ~600 K.[13] In addition, differently from layered manganites, the CO in $La_{1.5}Sr_{0.5}CoO_4$ is independent of magnetic order and compared to isostructural $La_{1.5}Sr_{0.5}MnO_4$ the CO results in a stronger charge localization. The CO state has been found also for other compositions around $x=0.50$ (Ref. 14) by means of elastic neutron scattering experiments. Regarding the magnetic transition temperature, increasing the Sr doping (from $x=0.50$) leads to a progressive reduction in the T_N corroborating the interpretation that the Co^{3+} are magnetically nonactive ions.[14]

A transition from HS Co^{3+} to LS Co^{3+} for $x\geq 0.4$, which accounts for the anisotropic susceptibility found in the series has instead being recently proposed.[14,15] Co^{2+} is usually considered in its high-spin state while Co^{4+} in the low-spin state.[14–16]

It is clear that spin and oxidation state may largely influence both structural and transport properties of these materials, as already seen for other Co-containing systems.[17–19] This is a consequence of the fact that the different oxidation and spin states are characterized by different sizes and tendencies to promote a Jahn-Teller distortion. Concerning the transport properties, it has been proposed for this[12] and other systems[20] that spin-blockade phenomena—i.e., the possibility that spins may affect charge motion to the extreme of severely suppressing the conductivity—can take place when Co is present in certain electronic configurations.

The structural properties of the solid solution $La_{2-x}Sr_xCoO_{4\pm\delta}$ have been studied, for different compositional ranges,[7,8,21] mainly at room temperature; high-temperature diffraction data are reported for the La_2CoO_4 end member[22] while low-temperature and high-pressure structural data have been studied for the composition $La_{0.6}Sr_{1.4}CoO_4$.[7]

Cobalt containing perovskites (and layered systems) have recently attracted a wide interest for what concerns their properties above RT, where they have been proposed as good candidates for thermoelectric applications,[9] in catalysis,[3] as well as cathode materials in solid oxide fuel cells.[4] We have

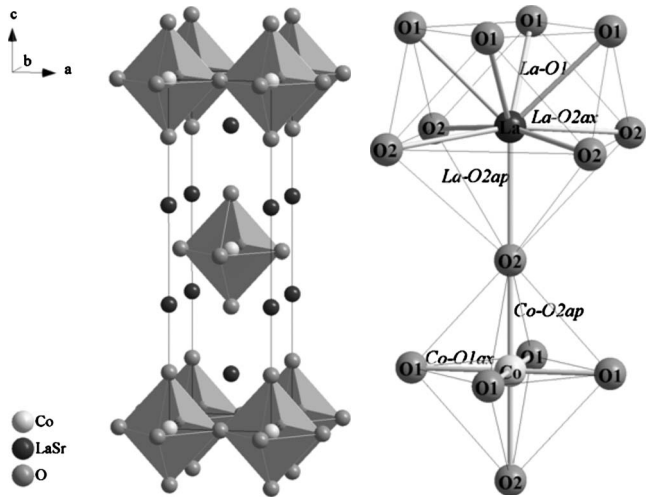

FIG. 1. Left panel: representation of the K_2NiF_4-type structure of $LaSrCoO_4$ showing the octahedral coordination around the B site and the layered nature of the structure. Right panel: representation of the cations coordination indicating the main cation-oxygen distances.

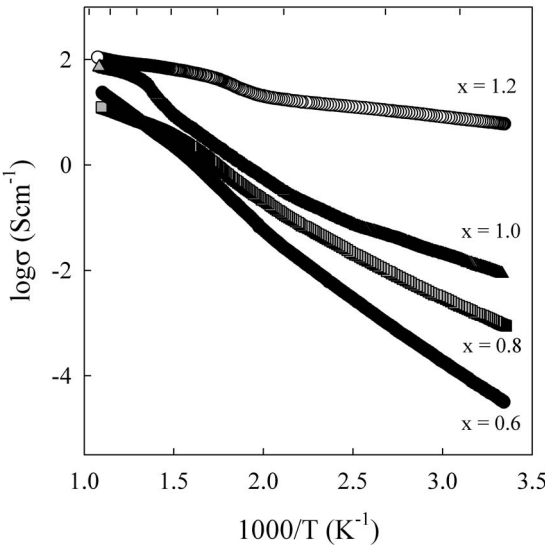

FIG. 2. Arrhenius plot of conductivity for $La_{2-x}Sr_xCoO_4$.

recently investigated the structure-properties correlation in related systems (e.g., $NdCoO_3$, $HoBaCo_2O_{5+\delta}$) with the aim of understanding the role of the different degrees of freedom (structure, Co oxidation state, Co spin state, and oxygen nonstoichiometry).[17,23] In order to deepen our understanding of the Co-containing single-layered perovskite system, we present here the investigation of the structural and transport properties of the solid solution $La_{2-x}Sr_xCoO_{4\pm\delta}$ $(0.6 \leq x \leq 1.2)$ as a function of temperature (RT–750 °C). This work represents the first systematic investigation of the $La_{2-x}Sr_xCoO_{4\pm\delta}$ $(0.6 \leq x \leq 1.2)$ solid solution in the high-temperature range which, for the reasons presented above, is needed in order to provide an essential piece of information in view of the possible applications of Co-containing perovskites.

II. EXPERIMENTAL

Powder samples of composition $La_{2-x}Sr_xCoO_{4\pm\delta}$ $(x=0.6;0.8;1.0;1.2)$ were prepared by a sol-gel modified Pechini method. Stoichiometric amounts of $La(NO_3)_3 \cdot 6H_2O$, $Sr(NO_3)_2$, and $Co(NO_3)_3 \cdot 6H_2O$ were used as starting materials, citric acid as the chelating agent and ethylene glycol to enhance the gelation process. A homogeneous aqueous solution of the metal salts was obtained after a thorough mixing. The pH of the solution was adjusted to approximately 8 in order to promote the complexation of the metal ions. The solution was dried slowly at 70 °C under continuous and vigorous stirring. After the complete evaporation of the water, the dried gel obtained was first heated at 700 °C to burn out the organic matter, then at 1300 °C for 12 h to improve the crystallization grade of the compound, and finally slowly cooled down to room temperature. Powder samples of composition $LaSrAlO_4$ and $LaSrGaO_4$ were prepared according to the same procedure.

Variable temperature high-resolution neutron diffraction data were acquired on the D1A instrument at the Institute Laue Langevin (ILL) in Grenoble in the temperature range 30–750 °C. The samples were placed in quartz tubes open to air inside a furnace and the diffraction pattern collected in the angular range 0°–160°, step 0.1°, wavelength 1.9095 Å. The diffraction patterns were analyzed according to the Rietveld method[24] by means of the FULLPROF software package.[25] The background due to the empty quartz tube (recorded at the same temperature of the sample) was subtracted from the pattern prior to refinement. Cell parameters, zero point, profile parameters, atomic positions, and thermal factors for all the ions were refined. Anisotropic thermal factors were used for the oxygen sites. Oxygen occupancies were refined for each composition as a function of temperature.

Direct current four probes conductivity measurements were performed in the temperature range 30–800 °C using a Solartron 1286 galvanostat/potentiostat.

III. RESULTS

Figure 2 shows the Arrhenius plot of the electrical conductivity for the four compositions under investigation. The conductivity behavior confirms a trend already observed in the literature:[16] in the low-temperature regime (RT–500 K) the activation energy decreases with the increase in the Sr content (calculated values between RT and 500 K are approximately 0.48 eV for $x=0.6$, 0.34 eV for $x=0.8$, 0.26 eV for $x=1.0$, and 0.07 eV for $x=1.2$). Above approximately 500 K, the conductivity plots strongly deviate from linearity, in particular, for La-rich samples, and the conductivities converge to similar values at high temperature (~900 K).

The conductivity values at room temperature are approximately 10 S cm^{-1} for $La_{0.8}Sr_{1.2}CoO_4$ and 10^{-2} S cm^{-1} for $La_{1.0}Sr_{1.0}CoO_4$, giving rise to a drop of almost 3 orders of magnitude in such a small compositional range. The conductivity at room temperature then decreases to 10^{-3} S cm^{-1} and 10^{-4} S cm^{-1} for $La_{1.2}Sr_{0.8}CoO_4$ and $La_{1.4}Sr_{0.6}CoO_4$, respectively.

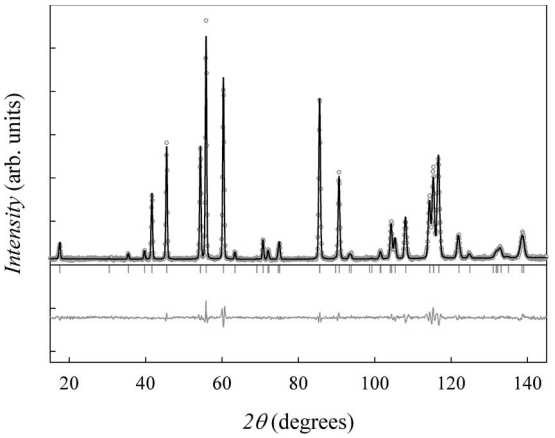

FIG. 3. Rietveld refined room-temperature neutron diffraction pattern of $La_{0.8}Sr_{1.2}CoO_4$ showing the observed (circles), calculated (black line), and difference profiles (gray line). Vertical bars refer to the Bragg peaks positions.

The neutron powder diffraction patterns of all samples at each investigated temperature can be unequivocally indexed in the tetragonal $I4/mmm$ space group. Figure 3 shows, as an example, the RT Rietveld-refined neutron diffraction pattern of $La_{0.8}Sr_{1.2}CoO_4$.

In Fig. 4 the evolution of the unit-cell parameters vs the Sr content at RT is reported. This graph shows that a decreases as the Sr content increases while the c parameter first decreases and then increases for $x>1$. This trend is consistent with previous reports on analogous compositions.[7] Figure 5 shows the evolution of the Co-O distances vs the Sr content. Both the Co-O1 (axial) and the Co-O2 (apical) distances decrease as the Sr content increases. The single La-O distances trend with composition is more complex with the La-O1 and La-O2ap distances increasing along with the Sr content whereas the La-O2ax distance is shortened (Fig. 6).

The first information that can be extracted from the analysis of the high-temperature neutron diffraction data is the absence of phase transitions for all the compositions in the

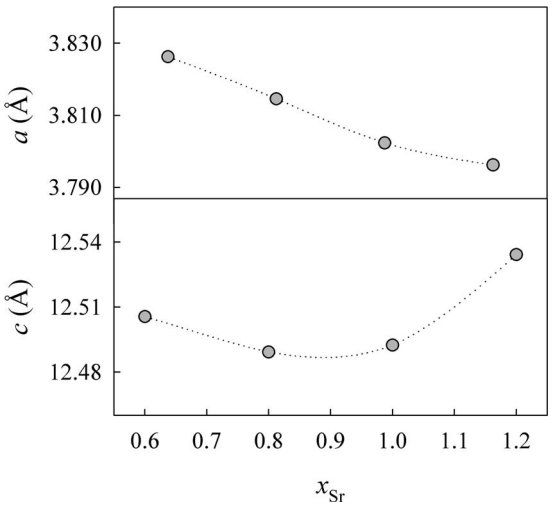

FIG. 4. Evolution of the unit-cell parameters vs composition for the $La_{2-x}Sr_xCoO_4$ series. Room temperature. The lines are only a guide for the eyes; error bars are smaller than the symbols.

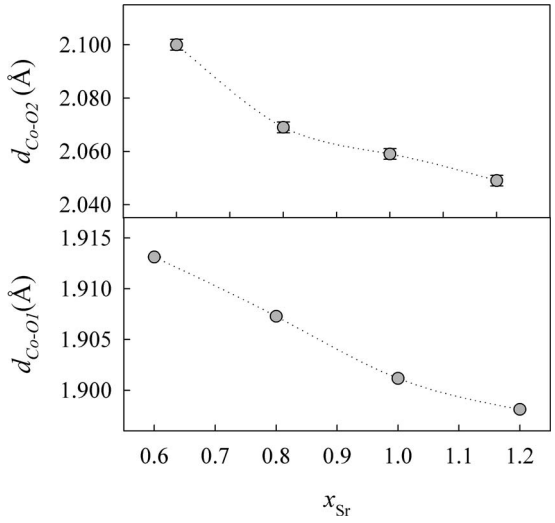

FIG. 5. Evolution of the Co-O distances vs composition for the $La_{2-x}Sr_xCoO_4$ series. Room temperature. The lines are only a guide for the eyes; when not visible, error bars are smaller than the symbols.

temperature range we explored. All of the diffraction patterns can be indexed in the tetragonal space group $I4/mmm$. The evolution of the unit-cell parameters with temperature (Fig. 7) shows a pronounced anisotropy in the thermal expansion. As a matter of fact, in the explored temperature range the parameters a and c change by 1.3% and 3.2%, respectively. Deviations from the linear trend are evidenced for each composition, with the exception of the $La_{0.8}Sr_{1.2}CoO_4$ sample,

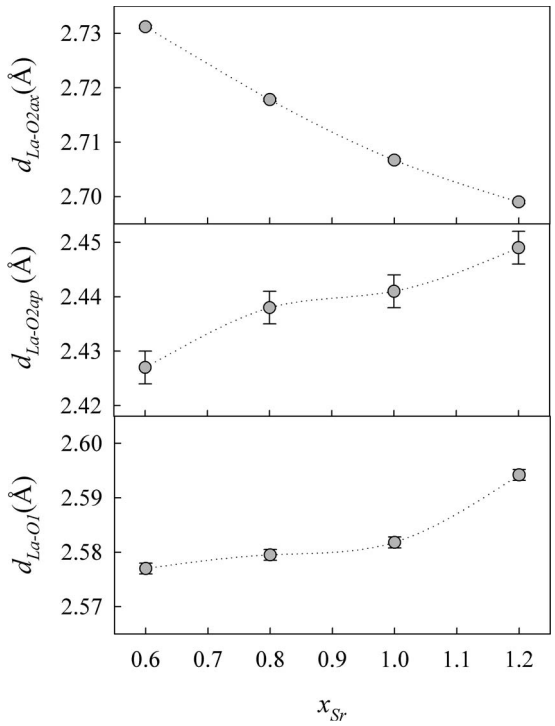

FIG. 6. Evolution of the La-O distances vs composition for the $La_{2-x}Sr_xCoO_4$ series. Room temperature. The lines are only a guide for the eyes; when not visible, error bars are smaller than the symbols.

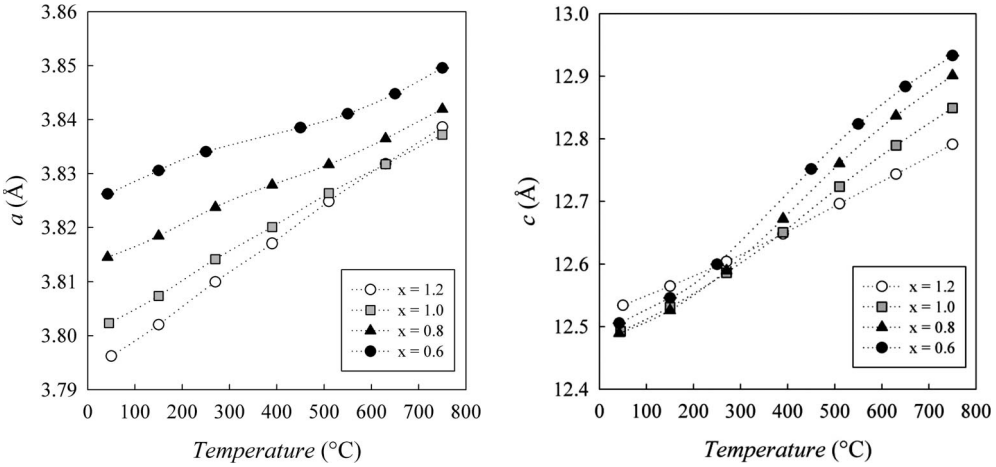

FIG. 7. Evolution of the unit-cell parameters vs temperature for $La_{2-x}Sr_xCoO_4$ showing the strong anisotropy in the thermal expansion. The lines are only a guide for the eyes; error bars are smaller than the symbols.

and these deviations are more pronounced as the Sr content decreases. The anomalous evolution of the unit-cell parameters with temperature are partially compensated in the unit-cell volume trend (Fig. 8), for which a slightly positive deviation is observed for decreasing Sr contents. Figure 9 shows the thermal expansion of the average cation-oxygen distances. The average ⟨La-O⟩ bond length expands almost linearly whereas for the ⟨Co-O⟩ bond length a positive deviation from linearity, which closely resembles the one found for the unit-cell volume (Fig. 8), is detected. More in detail, the analysis of the single Co-O distances (see Fig. 10) shows that $Co\text{-}O1_{eq}$ reproduces the *a* vs temperature trend whereas the $Co\text{-}O2_{ap}$ distance expands with a positive deviation from linearity which is more pronounced as the La content increases, as previously seen for the *c* parameter (Fig. 7). As a result, the distortion of the CoO_6 octahedra (calculated as the ratio between the apical Co-O2 and the axial Co-O1 distance) increases with temperature with increasing deviation from linearity as the Sr content decreases (Fig. 10). The octahedra are elongated along the *c* axis and the distortion decreases with the Sr content (Fig. 11).

IV. DISCUSSION

The results presented highlight that the trend of several structural parameters vs temperature for the $La_{2-x}Sr_xCoO_4$ series is complex and strongly dependent on composition. Already at room temperature a more complex behavior than the one expected on the basis of the simple change in the average ionic radius of the A site, due to the progressive substitution of Sr for La, is evidenced. In order to understand these results, it is not enough to consider only the change in the nominal composition on the A site of the structure. Instead, one has to realize that the aliovalent substitution on the A site has the primary effect of modifying the average oxidation state of Co, rather than appreciably changing the oxygen stoichiometry in order to maintain the same oxidation state on the B site of the structure. This effect, already dis-

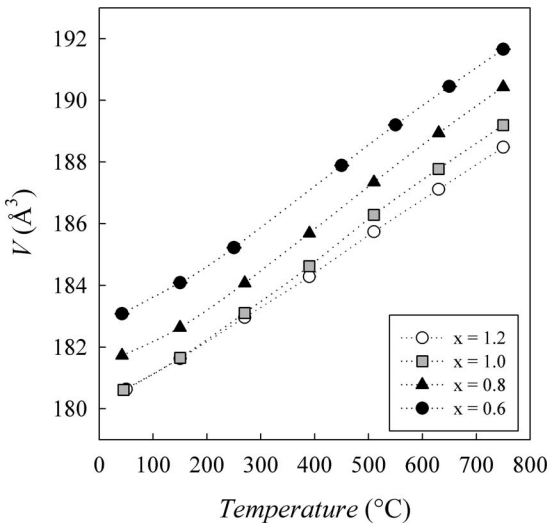

FIG. 8. Evolution of the unit-cell volume vs temperature for $La_{2-x}Sr_xCoO_4$. The lines are only a guide for the eyes; error bars are smaller than the symbols.

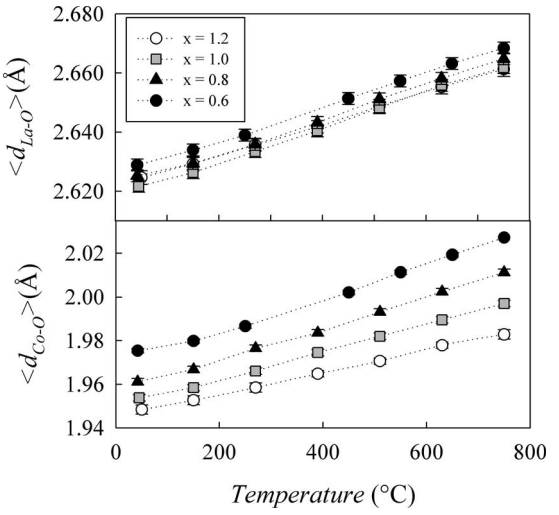

FIG. 9. Evolution of the average cation-oxygen bond lengths vs temperature for $La_{2-x}Sr_xCoO_4$. The lines are only a guide for the eyes; when not visible, error bars are smaller than the symbols.

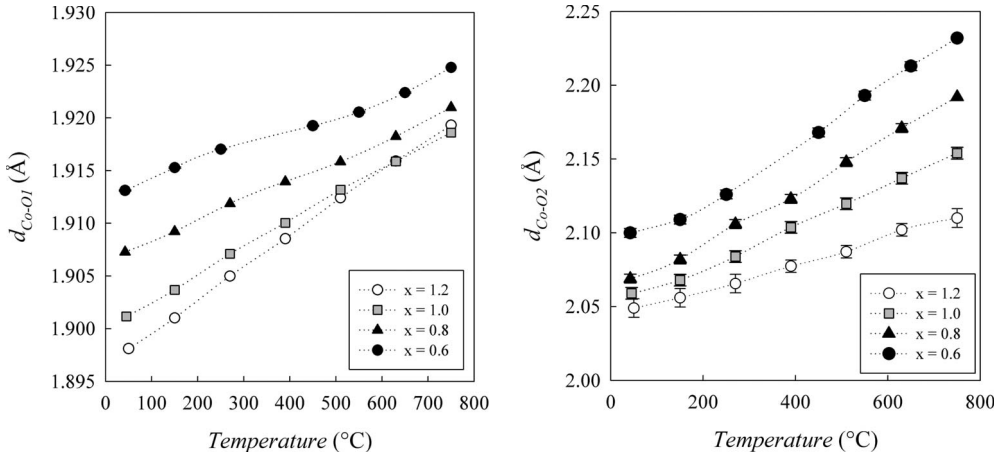

FIG. 10. Evolution of the single Co-O bond lengths vs temperature for $La_{2-x}Sr_xCoO_4$ showing the strong anisotropy in the thermal expansion: (a) Co-O1 axial distance (~1% variation); (b) Co-O2 apical distance (~10% variation). The lines are only a guide for the eyes; when not visible, error bars are smaller than the symbols.

cussed in the literature for analogous systems,[6,26] has been experimentally proven on our samples: in fact, Rietveld analysis of the oxygen occupancies showed that the oxygen content is very close to 4 for each composition, with values in excellent agreement with those reported in the literature for the same compositions[6] prepared under analogous synthesis conditions. Attempts to refine an interstitial oxygen position for La-rich samples were unsuccessful.

According to this Rietveld result, the average oxidation state of Co changes from approximately 2.60 to 3.10 as the Sr content increases from $x=0.6$ to $x=1.2$. This implies that while for the La-rich samples a portion of the Co is expected to be Co^{2+} for the $x=1.2$ sample Co^{4+} is present along with a large majority of Co^{3+}. Moreover, as stressed in Sec. I, Co can present different spin-state configurations along with different oxidation states, each characterized by a different size and a different tendency to promote Jahn-Teller distortion within the system.

The ionic radius of Co (HS configuration) in octahedral coordination varies according to the Co oxidation state, ranging from 0.745 Å for Co^{2+}, over 0.610 Å for Co^{3+} to 0.530 Å for Co^{4+}.[27] Within the same oxidation state the LS state has a smaller radius than the HS one (e.g., Co^{3+} in low-spin configuration has an ionic radius of 0.545 Å compared to the 0.610 Å of the high-spin state). Bearing in mind the relationship between the electronic configuration and the dimension of the transition-metal ion, it is possible to propose a model for the interpretation of the structural data vs composition. We have seen that the average oxidation state on the Co site increases from approximately 2.60 to 3.10 as the Sr content increases. An increase in the concentration of the smaller Co^{3+} and Co^{4+} over the larger Co^{2+} is expected to decrease the average ionic radius on the B site. This explains the shortening of the Co-O distances vs the Sr content (Fig. 5) and the same trend observed for the *a* lattice parameter (Fig. 4). As previously shown (Fig. 4), the *c* parameter displays a nonlinear behavior, reaching a minimum for $x=0.8$. This behavior can be interpreted as a result of two competing effects: the shortening of the Co-O apical distance, parallel to the *c* axis, and the increase in the average ionic radius on the A site as a consequence of the substitution of Sr for La, which is reflected in the increase in the La-O1 and La-O2 apical distances (Fig. 6), the last one being parallel to the *c* axis.

We recall here that these systems are supposed to conduct via small polaron hopping between charge carriers localized on the Co site mediated by oxygen atoms,[16] as for $LaCoO_3$. For a small polaron system, the hopping mechanism responsible for the electrical conductivity is favored when the hopping angle (in this case Co-O1-Co) is close to 180° and the Co-O distance is short. For our samples, all having tetragonal symmetry, the hopping angle is always 180° and therefore it cannot be a structural variable in the discussion. We can instead notice that, at room temperature, the Co-O1 distance decreases with the Sr content while the conductivity increases. In addition, at high temperature, where the conductivity of the samples converges to similar values, the Co-O distances do the same. This is a first indication of a possible

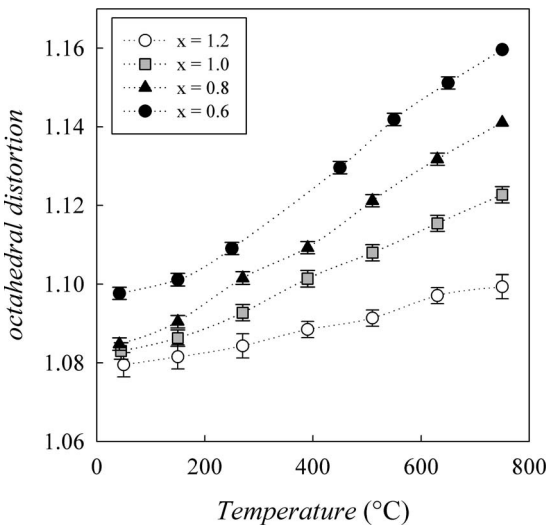

FIG. 11. Evolution of the octahedral distortion (defined as the ratio between the Co-O2 apical distance and the Co-O1 axial distance) vs temperature for $La_{2-x}Sr_xCoO_4$. The lines are only a guide for the eyes.

correlation between structural and transport properties for these materials, as already proposed for the $La_2(Ni,Co)O_{4\pm d}$ phases.[28]

However, the differences in the conductivity values observed at RT between the $La_{2-x}Sr_xCoO4$ samples and in the trend with temperature are too large to be attributed merely to a difference in the Co-O distance. The different electronic configurations of Co play certainly a role as well.

Rietveld analysis of the oxygen occupancies vs temperature showed that the oxygen content does not change significantly with temperature in the whole temperature range explored, which implies that the average oxidation state for Co is maintained for each composition at the value determined at room temperature. Therefore, we can conclude that the anomalous expansion behaviors found for several structural parameters cannot be ascribed to significant changes in the oxygen content and/or in the average Co oxidation state. We recall here that the loss of the interstitial oxygen with temperature in $La_2NiO_{4+\delta}$ had been shown to produce a regular expansion of the *a* parameter, and an anomalous contraction of the *c* parameter between 400 and 500 °C.[29] This had been related to the fact that interstitial oxygen is accommodated within these systems in the rocksalt layer, which is in contrast with the observed overexpansion of the *c* parameter for $La_{1.4}Sr_{0.6}CoO_4$ [Fig. 7].

In order to understand the behavior found in the $La_{2-x}Sr_xCoO_4$ system one has to consider that in Co containing samples, both the spin-state transitions and the disproportionation of Co^{3+} ions to Co^{2+} and Co^{4+} may be thermally activated, as reported for analogous systems.[30,31] There exists a rich literature on the $RECoO_3$ systems (*RE*=rare earth) which allows to discuss, on solid bases, the variation with composition and temperature of the Co spin states for the different Co oxidation states.[5,30] However, for the single-layered cobaltates, as discussed above, the situation regarding the investigation of the Co spin state and its dependence on physical properties and composition is far less known and, in some cases, conflicting reports have been reported (as for the $LaSrCoO_4$ system). Based on the available literature and on the data presented here, a possible explanation of the observed conductivity and structural properties evolution along with the Sr doping can, however, be proposed. In the doping range under investigation ($0.6 \leq x \leq 1.2$), and at room temperature, Co^{2+} ions is predicted to be in the HS state, Co^{3+} in the LS state, and Co^{4+} in the LS state, as proposed in the literature for $0.3 \leq x \leq 0.8$.[15] Figure 12(a) shows schematically the splitting and the occupation of the 3*d* levels for these ions. Temperature-induced spin-state transitions for the Co^{3+} ions [LS→IS, see Fig. 12(b)], as proposed for the $x < 0.8$ compositions,[13,15] may be present, and may influence both structural and transport properties. In addition, temperature-induced charge disproportionation of the IS Co^{3+} into Co^{2+} and Co^{4+}, as for the $LaCoO_3$ system, may not be ruled out and would further complicate the interpretation of the structural and transport properties. The onset of spin-state transition and charge disproportionation may also vary within the different compositions, as a consequence of the chemically induced pressure in the structure. (This scenario can partially explain the observed structural and transport properties). As shown in Fig. 12(a), charge transfer between

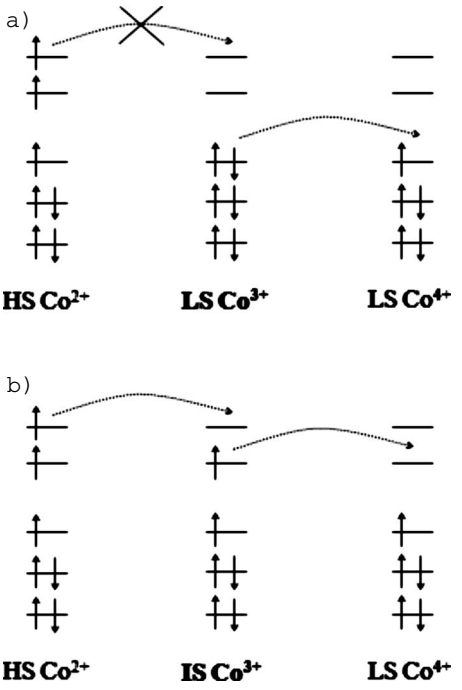

FIG. 12. Schematic representation of the splitting of the 3*d* levels showing the processes of charge transfer on the background of LS Co^{3+} and IS Co^{3+}.

HS Co^{2+} and LS Co^{3+} may be severely suppressed compared to charge transfer between LS Co^{3+} and LS Co^{4+} (for $x=1.2$), the first one being an example of spin blockade for electron hopping.[20] The nonlinear temperature dependence of conductivity, especially for the low Sr content, may be the effect of a progressive transition of the Co^{3+} ions from LS to a higher spin state, which would result in an improved charge transfer [Fig. 12(b)]. In addition, the proposed transition is consistent with a shifting of the charge from the t_{2g} level to the e_g level with consequent predicted elongation of the CoO_6 octahedra which could support our structural observations. This proposed scenario is also in agreement with the progressive reduction in the CoO_6 distortion along with the Sr doping, interpreted as a result of a reduction in the energy splitting between the d_{yz}, d_{zx}, and d_{xy} orbitals.[16] According to this model, questions remain open about the spin state of Co^{3+} for the $x=1.2$, since the very high conductivity at room temperature should then be attributed to the hopping of t_{2g} electrons, which is considered much weaker than that of e_g electrons.[20] If the spin state of the majority of the Co^{3+} ions for $x=1.2$ were IS already at room temperature, as proposed for $La_{0.5}Sr_{1.5}CoO_4$,[16] the higher conductivity of this sample—compared to the other samples—as well as its lower dependence on temperature, could be well interpreted. However, a spin-state transition from LS to IS along with the Sr doping has never being proposed in the literature up to now.

We recognize that the model proposed here in order to describe the trend of the $La_{2-x}Sr_xCoO_{4\pm\delta}$ ($0.6 \leq x \leq 1.2$) solid solution along with the Sr doping and temperature is plausible and based on the data presented here together with the literature results. We stress that further spectroscopic and magnetic measurements are needed in order to confirm this

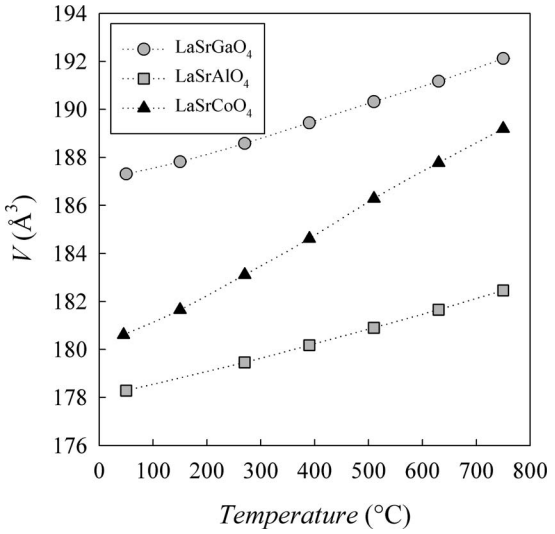

FIG. 13. Evolution of the unit-cell volume vs temperature for $LaSrBO_4$ (B=Al,Co,Ga). The lines are only a guide for the eyes; error bars are smaller than the symbols.

picture, both as a function of composition for the $x>1$ region and as a function of temperature. As a matter of fact, inelastic neutron scattering and electron spin resonance measurements in the $LaCoO_3$ system[32] have shown that the spin-state transition occurring around 100 K from a LS state of Co^{3+} could be interpreted in terms of a LS to HS spin-orbit triplet as the first excited state instead of LS to IS (as usually thought). So it is clear that even a possible spin-orbit coupling could not be ruled out in any of these Co-containing systems but the precise identification of the spin-state transition requires additional experimental evidences which go beyond the scope of the present work.

To support the main result of this study, i.e., the strong influence of the Co ion degrees of freedom (oxidation and spin states) on the structural properties of K_2NiF_4-type oxides, Fig. 13 compares the evolution of the unit-cell volume with temperature of $LaSrAlO_4$, $LaSrGaO_4$, and $LaSrCoO_4$. From this figure the linear trend of the unit-cell volume with temperature is appreciable for the Al and Ga compounds, in contrast to the more complex behavior found for $LaSrCoO_4$, which also shows a larger percentage variation (~4% instead of ~2%) in the explored temperature range.

V. CONCLUSIONS

This study focuses on the characterization, in a wide temperature range, of the structural and transport properties of the $La_{2-x}Sr_xCoO_4$ solid solution. The temperature range investigated (30–750 °C) is of particular interest in view of the potential applications of this class of materials as catalysts and cathode material for intermediate-temperature solid oxide fuel cells.

The results indicate that the trend of several structural parameters as a function of temperature for the $La_{2-x}Sr_xCoO_4$ series is complex and strongly dependent on composition with peculiar deviation from linearity in particular for La-rich samples. High conductivity values and low activation energy have been found for the $La_{0.8}Sr_{1.2}CoO_4$ composition. Considerably lower conductivity values are found for $x<1.0$ at room temperature; a strong dependence upon temperature makes the differences between the four samples less pronounced at high temperature (>450 °C), but the $La_{0.8}Sr_{1.2}CoO_4$ composition retains the higher conductivity in the whole temperature range.

A correlation between structural and transport properties, based on changes in the average oxidation and spin state of the Co ions, can be proposed. A final detailed understanding of these phenomena is difficult to achieve as they are the result of a fine balance between several structural and electronic aspects.

ACKNOWLEDGMENTS

Financial support from the Cariplo Foundation and the INSTM-Regione Lombardia project is gratefully acknowledged.

*Corresponding author. FAX: +39.0382.987575; cristina.tealdi@unipv.it

[1] J. G. Bednorz and K. A. Müller, Z. Phys. B: Condens. Matter **64**, 189 (1986).
[2] C. W. Chu, P. H. Hor, R. L. Meng, L. Gao, and Z. J. Huang, Science **235**, 567 (1987).
[3] L. Borovskikh, G. Mazo, and E. Kemnitz, Solid State Sci. **5**, 409 (2003).
[4] A. Tarancón, M. Burriel, J. Santiso, S. J. Skinner, and J. A. Kilner, J. Mater. Chem. **20**, 3799 (2010).
[5] J. B. Goodenough, Rep. Prog. Phys. **67**, 1915 (2004).
[6] V. Vashook, H. Ullmann, O. P. Olschevskaya, V. P. Kulik, M. E. Lukaschevich, and L. V. Kochanovskij, Solid State Ionics **138**, 99 (2000).
[7] A. V. Chichev, M. Dlouhá, S. Vratislav, K. Knížek, J. Hejtmánek, M. Maryško, M. Veverka, Z. Jirák, N. O. Golosova, D. P. Kozlenko, and B. N. Savenko, Phys. Rev. B **74**, 134414 (2006).
[8] Y. Moritomo, K. Higashi, K. Matsuda, and A. Nakamura, Phys. Rev. B **55**, R14725 (1997).
[9] R. Ang, Y. P. Sun, X. Luo, C. Y. Hao, and W. H. Song, J. Phys. D **41**, 045404 (2008).
[10] H. Wu, Phys. Rev. B **81**, 115127 (2010).
[11] J. Wang, W. Zhang, and D. Y. Xing, Phys. Rev. B **62**, 14140 (2000).
[12] C. F. Chang, Z. Hu, H. Wu, T. Burnus, N. Hollmann, M. Benomar, T. Lorenz, A. Tanaka, H.-J. Lin, H. H. Hsieh, C. T. Chen, and L. H. Tjeng, Phys. Rev. Lett. **102**, 116401 (2009).
[13] I. A. Zaliznyak, J. M. Tranquada, R. Erwin, and Y. Morimoto, Phys. Rev. B **64**, 195117 (2001).
[14] M. Cwik, M. Benomar, T. Finger, Y. Sidis, D. Senff, M. Reuther, T. Lorenz, and M. Braden, Phys. Rev. Lett. **102**, 057201 (2009).
[15] N. Hollmann, M. W. Haverkort, M. Cwik, M. Benomar, M. Re-

uther, A. Tanaka, and T. Lorenz, N. J. Phys. **10**, 023018 (2008).
[16] T. Matsuura, J. Tabichi, J. Mizusaki, S. Yamauchi, and K. Fueki, J. Phys. Chem. Solids **49**, 1403 (1988); **49**, 1409 (1988).
[17] C. Tealdi, L. Malavasi, F. Gozzo, C. Ritter, M. C. Mozzati, G. Chiodelli, and G. Flor, Chem. Mater. **19**, 4741 (2007).
[18] P. G. Radaelli and S. W. Cheong, Phys. Rev. B **66**, 094408 (2002).
[19] C. Frontera, J. L. Garcia-Munoz, A. E. Carrillo, M. A. G. Aranda, I. Margiolaki, and A. Caneiro, Phys. Rev. B **74**, 054406 (2006).
[20] A. Maignan, V. Caignaert, B. Raveau, D. Khomskii, and G. Sawatzky, Phys. Rev. Lett. **93**, 026401 (2004).
[21] X. Yang, L. Luo, and H. Zhong, Appl. Catal., A **272**, 299 (2004).
[22] A. Aguadero, J. A. Alonso, and L. Daza, Z. Naturforsch. B **63**, 615 (2008).
[23] Y. Diaz-Fernandez, L. Malavasi, and M. C. Mozzati, Phys. Rev. B **78**, 144405 (2008).
[24] H. M. Rietveld, Acta Crystallogr. **22**, 151 (1967); J. Appl. Crystallogr. **2**, 65 (1969).
[25] J. Rodriguez-Carvajal, Physica B **192**, 55 (1993).
[26] H. Taguchi, Solid State Sci. **9**, 869 (2007).
[27] D. Shannon, Acta Crystallogr., Sect. A: Cryst. Phys., Diffr., Theor. Gen. Crystallogr. **32**, 751 (1976).
[28] S. J. Skinner and G. Amow, J. Solid State Chem. **180**, 1977 (2007).
[29] S. J. Skinner, Solid State Sci. **5**, 419 (2003).
[30] M. A. Senaris-Rodriguez and J. B. Goodenough, J. Solid State Chem. **118**, 323 (1995).
[31] S. R. Sehlin, H. U. Anderson, and D. M. Sparlin, Phys. Rev. B **52**, 11681 (1995).
[32] A. Podlesnyak, S. Streule, J. Mesot, M. Medarde, E. Pomjakushina, K. Conder, A. Tanaka, M. W. Haverkort, and D. I. Khomskii, Phys. Rev. Lett. **97**, 247208 (2006).